

Alterations in cerebral and cardiac mitochondrial function in a porcine model of acute carbon monoxide poisoning

David H. Jang , Sarah Piel , John C. Greenwood , Matthew Kelly , Vanessa M. Mazandi , Abhay Ranganathan , Yuxi Lin , Jonathan Starr , Thomas Hallowell , Frances S. Shofer , Wesley B. Baker , Alec Lafontant , Kristen Andersen , Johannes K. Ehinger & Todd J. Kilbaugh

To cite this article: David H. Jang , Sarah Piel , John C. Greenwood , Matthew Kelly , Vanessa M. Mazandi , Abhay Ranganathan , Yuxi Lin , Jonathan Starr , Thomas Hallowell , Frances S. Shofer , Wesley B. Baker , Alec Lafontant , Kristen Andersen , Johannes K. Ehinger & Todd J. Kilbaugh (2021): Alterations in cerebral and cardiac mitochondrial function in a porcine model of acute carbon monoxide poisoning, *Clinical Toxicology*, DOI: [10.1080/15563650.2020.1870691](https://doi.org/10.1080/15563650.2020.1870691)

To link to this article: <https://doi.org/10.1080/15563650.2020.1870691>



Published online: 02 Feb 2021.



Submit your article to this journal [↗](#)



Article views: 28



View related articles [↗](#)



View Crossmark data [↗](#)

BASIC RESEARCH



Alterations in cerebral and cardiac mitochondrial function in a porcine model of acute carbon monoxide poisoning

David H. Jang^a , Sarah Piel^b, John C. Greenwood^c, Matthew Kelly^d, Vanessa M. Mazandi^b, Abhay Ranganathan^b, Yuxi Lin^b, Jonathan Starr^b, Thomas Hallowell^b, Frances S. Shofer^a, Wesley B. Baker^e, Alec Lafontant^e, Kristen Andersen^e, Johannes K. Ehinger^{f,g}  and Todd J. Kilbaugh^b 

^aDepartment of Emergency Medicine, Division of Medical Toxicology, University of Pennsylvania School of Medicine, Philadelphia, PA, USA; ^bResuscitation Science Center, Philadelphia, PA, USA; ^cDepartment of Anesthesiology and Critical Care Medicine, Department of Emergency Medicine, University of Pennsylvania School of Medicine, Philadelphia, PA, USA; ^dDepartment of Emergency Medicine, University of Alabama at Birmingham, Birmingham, AL, USA; ^eDepartment of Pediatric Neurology, The Children's Hospital of Philadelphia (CHOP), Philadelphia, PA, USA; ^fMitochondrial Medicine, Department of Clinical Sciences Lund, Lund University, Lund, Sweden; ^gDepartment of Otorhinolaryngology, Head and Neck Surgery, Skåne University Hospital, Lund University, Malmö, Sweden.

ABSTRACT

Objectives: The purpose of this study is the development of a porcine model of carbon monoxide (CO) poisoning to investigate alterations in brain and heart mitochondrial function.

Design: Two group large animal model of CO poisoning.

Setting: Laboratory.

Subjects: Ten swine were divided into two groups: Control ($n = 4$) and CO ($n = 6$).

Interventions: Administration of a low dose of CO at 200 ppm to the CO group over 90 min followed by 30 min of re-oxygenation at room air. The Control group received room air for 120 min.

Measurements: Non-invasive optical monitoring was used to measure cerebral blood flow and oxygenation. Cerebral microdialysis was performed to obtain semi real time measurements of cerebral metabolic status. At the end of the exposure, both fresh brain (cortical and hippocampal tissue) and heart (apical tissue) were immediately harvested to measure mitochondrial respiration and reactive oxygen species (ROS) generation and blood was collected to assess plasma cytokine concentrations.

Main results: Animals in the CO group showed significantly decreased Complex IV-linked mitochondrial respiration in hippocampal and apical heart tissue but not cortical tissue. There also was a significant increase in mitochondrial ROS generation across all measured tissue types. The CO group showed a significantly higher cerebral lactate-to-pyruvate ratio. Both IL-8 and TNF α were significantly increased in the CO group compared with the Control group obtained from plasma. While not significant there was a trend to an increase in optically measured cerebral blood flow and hemoglobin concentration in the CO group.

Conclusions: Low-dose CO poisoning is associated with early mitochondrial disruption prior to an observable phenotype highlighting the important role of mitochondrial function in the pathology of CO poisoning. This may represent an important intervenable pathway for therapy and intervention.

ARTICLE HISTORY

Received 11 November 2020

Revised 16 December 2020

Accepted 25 December 2020

KEYWORDS

CNS/psychological; organ/tissue specific; complications of poisoning; metabolic; complications of poisoning; other

Introduction

Carbon monoxide (CO) is a colorless and odorless gas that is an important cause of poisoning mortality and morbidity in the United States with approximately 15,000 intentional cases annually accounting for over two-thirds of reported deaths [1]. Specifically, there are over 50,000 CO cases seen in emergency departments in the US annually, with over half requiring hospitalization [2]. It is estimated that CO poisoning results in over \$1 billion annually in hospital costs and lost earnings [3]. The most serious complications for survivors of consequential CO exposure is neurologic morbidity with delayed neurological sequelae (DNS) occurring in up to 50% of patients [4]. While the neurological morbidity is well

known, less is known about the cardiac involvement for patients exposed to CO [5]. There is some evidence to suggest temporary cardiac dysfunction in victims of acute CO poisoning, there is also evidence to suggest more long-term effects. In most cases, the cellular underpinning resulting in possible cardiac dysfunction is not clear [6]. The mechanism of CO poisoning is complex that includes hypoxia, inflammation and lipid peroxidation. Another important mechanism of cellular injury includes mitochondrial dysfunction [7]. CO targets cytochrome c oxidase or Complex IV (CIV) resulting in bioenergetic failure and propagation of reactive oxygen species (ROS) leading to organ dysfunction. Our work has implicated the emerging role the mitochondria may have in CO poisoning [8–10].

The mitochondria perform multiple essential functions beyond energy production and may be the final regulator determining cellular fate following injury and poisoning [11]. Mitochondria play a central role in cellular metabolism where oxygen (O_2) consumption through the mitochondrial electron transport system (ETS) is tightly coupled to ATP production and is regulated by metabolic demand [12]. Failure of the mitochondria to use O_2 to sustain ATP production results in an energy deficit that can impair cell function [13–15]. Decreased ETS activity and low ATP levels in muscle biopsies have also been linked to death in other forms of shock such as sepsis and traumatic injuries [16]. The maintenance of mitochondrial function is crucial to cellular health.

While there are numerous small animal models of CO poisoning, there is a paucity of large animal models to study cellular dysfunction and potential future therapy in CO poisoning [17]. Additionally, many agencies that oversee toxicological testing require use of both rodent and non-rodent species [18]. In general toxicology testing, dogs and non-human primates are used as non-rodent models. However, there are numerous instances where the swine are the ideal translational model of biomedical research because of anatomical, physiological, and biochemical similarity to humans and swine are considered a suitable animal model for cardiovascular and neural disease [19]. Other obvious advantages of a large animal model include serial blood draws and more sophisticated monitoring that better mimic the clinical setting with patients with CO poisoning.

The primary objective of this study was to establish a porcine model of acute CO poisoning to determine effects on mitochondrial function in brain and heart tissue. Our prior work shows that the mitochondria may play a critical role in CO poisoning and represent an important area for monitoring and therapy [10]. In addition, we employed cerebral microdialysis (cMD) to assess semi real-time changes in cerebral metabolism and non-invasive optical monitoring for both cerebral blood flow and oxygenation along with measures of inflammation in blood.

Material and methods

Animals and overall study design

All procedures were approved by the Institutional Animal Care and Use Committee at the Children's Hospital of Philadelphia and performed in accordance with the National Institutes of Health Guide for the Care and Use of Laboratory Animals. 9-week-old Yorkshire pigs ($n=10$; mean weight 20 kg) were premedicated with 20 mg/kg ketamine, followed by inhaled isoflurane in 100% oxygen *via* a snout mask. They were then intubated as described below, and oxygen was weaned to room air. The animals were randomized to two different treatment groups: Control ($n=4$) and Carbon monoxide ($n=6$).

Perioperative procedures and monitoring

Ventilator settings were as follows: tidal volume 10–11 ml/kg, positive end-expiratory pressure 5 cm H_2O and respiratory

rate titrated to achieve end-tidal carbon dioxide 35–45 mmHg to minimize potential confounding changes in cerebral blood flow and acid–base status. The right femoral artery and vein were cannulated for arterial pressure monitoring and central venous access. Isoflurane was weaned to approximately 0.5–1% to simulate human anesthetic protocols and minimize confounding toxicity and cerebral blood flow changes associated with higher doses of isoflurane. A rectal temperature probe was placed. All data were recorded with PowerLab 16/35 LabChart 8 Pro software from ADInstruments (Sydney, Australia).

Carbon monoxide experimental protocol

An endobronchial tube (Left) 32 Fr/Ch (10.7 mm) from Covidien (Owned by Medtronic in Dublin, Ireland) was used to intubate each animal. The 32 Fr tracheal lumen was connected to the vent and the bronchial lumen was attached to the CO tank described below. Only the tracheal cuff (7 cc) was inflated, and the bronchial cuff was left deflated to allow the passage of CO. A concentration of 200 ppm of CO was administered with a 200 ppm CO tank 244 cf using a Regulator 0–10 L/min with flow meter from Airgas (Radnor Township, PA, USA). The CO concentration entering the endobronchial tube was monitored using an Inspector CO detector with a 0–2000 ppm range (Sensorcon, New York, USA). Animals in the CO group received CO at the 200 ppm for 90 min followed by 30 min of room air to mimic removal of subjects from a CO exposure. Animals in the Control group received 120 min of room air. All animals were maintained on inhaled isoflurane for the duration of the procedure.

Non-invasive measurement of cerebral blood flow and oxygenation

Non-invasive neuromonitoring comprising frequency-domain diffuse optical spectroscopy (FD-DOS) and diffuse correlation spectroscopy (DCS) was placed and secured following anesthetic induction and intubation [20,21]. FD-DOS/DCS measurements were acquired in the left frontal cortex *via* a non-invasive optical probe sutured to the left forehead. Multi-distance FD-DOS was used to continuously measure cerebral tissue oxygen saturation (StO_2 , %) and oxygen extraction fraction (OEF). FD-DOS employs radio-frequency intensity-modulated near-infrared light to quantify wavelength-dependent absorption and scattering properties of tissue. A customized, commercial instrument (Imagent, ISS Inc.), equipped with three 690, 725, and 830 nm intensity-modulated (110 MHz) diode laser sources and two photomultiplier tube detectors, was coupled to the fiber optic probe; source-detector separations ranged from 0.75 cm to 3 cm. For each subject, the source- and detector-fiber coupling coefficients to the tissue were estimated using a phantom-calibration approach and used to correct continuous (10 Hz) AC intensity and phase data. Using a multi-distance linear fitting method, absolute absorption and scattering coefficients were calculated for each wavelength from these data. Coefficients were

excluded if the linear fit Pearson correlation coefficient was <0.95 , and the data-point excluded if more than one of the four scattering or absorption coefficients were excluded [22].

DCS is an optical method based on dynamic light scattering, which analyzes temporal fluctuations of light transmitted through tissue. As red blood cells are the primary light scattering objects moving within tissue, DCS allows measurement of the cerebral blood flow (CBF). A 785 nm long-coherent length (~ 10 m) laser (Toptica; RCL-080-785-S, Farmington, NY) was coupled to a multimode (62.5/125 μm) optical source fiber to transport light to the tissue. Two four-channel single photon counting modules (SPCM-AQ4C; Excelitas Technologies, Corp., Watltham, MA) registered the scattered light that was brought back from the tissue by eight single mode detector fibers (core diameter ~ 5 μm). Two different source-detector separations were used – two separations of 1.69 cm and six separations of 2.44 cm. A real-time software correlator was implemented using an 8 channel PCIe/PXIe6612 counter/timer data acquisition board (LabVIEW; National Instruments, Austin, TX) which computed an autocorrelation function of scattered light intensity based on photon arrival times. This correlator has a data acquisition rate of 20 Hz, allowing for assessment of flow pulsatility [23].

Measurement of cerebral microdialysis

Cerebral microdialysis (cMD) allows bedside semicontinuous monitoring of brain extracellular fluid. cMD was placed in the left frontal cortex using a CMA 70 Elite from mDialysis (Stockholm, Sweden). Probes were placed 0.5–1 cm deep in the brain parenchyma. Sterile saline was perfused at 1 $\mu\text{l}/\text{min}$, and after a 30 min calibration period, samples were collected in 30 min intervals throughout the CO exposure and reoxygenation. Samples were immediately frozen at -80°C . Pyruvate, lactate, glycerol and glucose concentrations were analyzed in a blinded fashion using the automated ISCUS FlexTM Microdialysis Analyzer and data were processed using the ICU-pilot software from mDialysis (Stockholm, Sweden).

Tissue extraction and preparation

Upon completion of the protocol described above, all subject animals were euthanized with an overdose of potassium chloride (KCl) after which the brain (cortex and hippocampus regions) and heart tissue (apex of left ventricle) were immediately obtained. Both brain and heart immediately underwent rapid but gentle dissection and were then immediately transferred into ice-cold buffer solution (320 mM sucrose, 2 mM EGTA, 10 mM Trizma base, pH 7.4). The brain tissue was weighed and manually homogenized in a 5-mL Potter-Elvehjem teflon-glass homogenizer to obtain a concentration of 1 mg wet weight tissue/1 mL MIR05 buffer (0.5 mM EGTA, 3 mM MgCl_2 , 60 mM K-lactobionate, 20 mM Taurine, 10 mM KH_2PO_4 , 20 mM HEPES, 110 mM sucrose, 1 g/L BSA, pH 7.1), 200–300 mg of heart tissue (apex) was transferred to ice-cold Buffer A (100 mM KCl, 50 mM MOPS, 100 ml of 10 mM EGTA, pH 7.4) and manually homogenized following a 30 min incubation with trypsin (10 mg per sample). Subsequently

mitochondria were isolated by differential centrifugation and application of density gradients using Percoll. Brain tissue homogenate and isolated heart mitochondria immediately underwent measurement of mitochondrial respiration and ROS production [24,25].

Measurement of mitochondrial respiration

Mitochondrial respiratory function was analyzed specifically in the tissue obtained above using multiple Oroboros O2k-FluoRespirometers (Oroboros Instruments, Innsbruck, Austria) with a substrate–uncoupler–inhibitor titration (SUIT) protocol as previously described in our work [11,24,25]. The SUIT protocol measures oxidative phosphorylation capacity with electron flow through both complex I (CI) and complex II (CII) respectively, and the convergent electron input (CI + CII) using the nicotinamide adenine dinucleotide-linked substrates, malate (5 mM) and pyruvate (5 mM) and glutamate (5 mM), as well as the flavin adenine dinucleotide-linked substrate succinate (10 mM), both in the presence of adenosine diphosphate (1 mM). Oxidative phosphorylation produces adenosine triphosphate (ATP), which is the primary fuel for performing basic function. During times of stress and injury, increased maximal oxidative phosphorylation is necessary for neuronal salvage and repair because of high-energy requirements. Oligomycin, an inhibitor of the ATP synthase, uncouples respiration from ATP-synthase activity to measure respiration where the O_2^- consumption is dependent on the leakiness the mitochondrial membrane and back-flux of protons into the mitochondrial matrix that is independent of the ATP synthase ($\text{LEAK}_{\text{CI}+\text{CII}}$). If LEAK respiration is increased, the electrochemical gradient across the mitochondrial membrane is uncoupled, resulting in inadequate ATP production. Maximal convergent non-phosphorylating respiration of $\text{ETS}_{\text{CI}+\text{CII}}$ is evaluated by titrating the protonophore, carbonyl cyanide p-(trifluoromethoxy) phenylhydrazone. $\text{ETS}_{\text{CI}+\text{CII}}$ is considered a stress test for the mitochondria, as a marker of mitochondrial respiratory reserve. Non-phosphorylating respiration through CII (ETS_{CII}) is achieved through the addition of rotenone (2 mM). The CIII inhibitor antimycin-A (5 mM) is added to measure the residual non-mitochondrial oxygen consumption, and this value was subtracted from each of the measured respiratory states to provide only mitochondrial respiration. CIV-linked respiration was measured by the addition of N,N,N-tetramethyl-phenylenediamine (0.5 mM) together with ascorbate (0.8 mM). The CIV inhibitor sodium azide (10 mM) was added to reveal the chemical background that is subtracted from the N,N,N-tetramethyl-phenylenediamine-induced oxygen consumption rate. Our previous works describe measuring CIV-linked respiration in the setting of CO poisoning [8,9]. Brain cortex and hippocampus regions were normalized to citrate synthase activity and isolated mitochondria from heart tissue were expressed μg protein count obtained with a Pierce BCA Protein Assay kit (catalog 23227) from Thermo Fisher Scientific (Waltham, MA, USA). All data were acquired using DatLab 7 (Oroboros Instruments, Innsbruck, Austria).

Measurement of reactive oxygen species in brain and heart tissue

Measurements of ROS generation as hydrogen peroxide (and converted superoxide) was measured using the O2k-Fluorescence LED2-Module attached to the Oroboros O2k-FluoRespirometer, permitting simultaneous measurements of hydrogen peroxide (H₂O₂) production and mitochondrial respiration, utilizing an Amplex UltraRed assay as previously described [9]. In short, Amplex UltraRed (N-acetyl-3, 7 dihydroxyphenoxazine) (5 mM), in the presence of horseradish peroxidase (1 U/ml), reacts with H₂O₂ to produce the fluorescent compound resorufin. The addition of superoxide dismutase (SOD) (10 U/ml) ensures that all superoxide is converted into H₂O₂. A 3-point calibration of the fluorometric signal was done prior to each measurement by the addition of 100 nM H₂O₂. Mitochondrial ROS generation is the predominant source of ROS and leads to alterations in redox signaling, oxidative damage to proteins and lipids, additional mitochondrial dysfunction and ultimately a major cause of ongoing secondary brain and heart injury.

Measurement of inflammation

Plasma was isolated by centrifugation and evaluated by multiplex enzyme immunoassay using the Q-Plex Porcine Cytokine Panel (4-Plex) using a multiplex ELISA Quansys Biosciences (Logan, Utah, USA) for the cytokine interleukin 1 β (IL-1 β ; Pro-Tumor Inflammation), interleukin-6 (IL-6; a pro-inflammatory cytokine), interleukin-8 (IL-8; an inflammatory cytokine), and tumor necrosis factor (TNF α ; inflammatory cytokine and acute phase reactant).

Citrate synthase activity

Citrate synthase activity (CS) was measured as a marker of mitochondrial content and used in addition to tissue weight for normalization of brain tissue as previously described [24]. Chamber contents from the brain high-resolution respirometry measurements were frozen for subsequent CS activity measurements. A commercially available kit (Citrate Synthase Assay Kit, CS0720, Sigma-Aldrich, St Louis, MO, USA) was used according to the manufacturer's instructions to determine the CS activity (μ mol/ml/min).

Statistics and data analysis

This was a pilot developmental study for feasibility of doing the experiment. Based on our previous work in this area we were looking for large differences, with effect sizes on the order of 2.0 or larger that is reflected in the number of animals. Statistics were calculated by using GraphPad Prism version 8.0.0 for Mac, GraphPad Software (San Diego, CA, USA). Data are presented as mean \pm SEM if not indicated otherwise. Differences between groups were assessed using analysis of variance in repeated measures. Post-hoc pair wise comparisons using Tukey Kramer t-tests to adjust for multiple comparisons were used to assess differences between groups

Table 1. Group characteristics at post 2-h exposure.

Group characteristics			
Variable	Control (n = 4)	CO (n = 6)	p-Value
Weight (kg)	20.5 (1.33)	20.7 (1.35)	0.81
<i>Blood Gases</i>			
pH	7.46 (0.02)	7.49 (0.07)	0.31
PaCO ₂ (mmHg)	47 (2.5)	46.5 (4.73)	0.85
Lactate (mmol/l)	1.25 (0.37)	0.83 (0.17)	0.06
COHb (%)	0.45 (0.38)	10.1 (1.47)	0.00001
<i>Hemodynamics</i>			
Heart rate (bpm)	114 (7.99)	142 (12.07)	0.025
Mean arterial pressure (mmHg)	67 (5.45)	59 (7.73)	0.13

All values are represented as mean (SD).

There were no baseline differences in any of the variable reported obtained prior to the 2-h exposure. All values expressed mean (SD). PaCO₂: partial pressure of arterial carbon dioxide.

and respiratory states. Data were checked for normality using the Shapiro-Wilks normality test. All variables did not deviate significantly from normal with p -values $>.10$. A p value of <0.05 was considered statistically significant.

Result

Baseline characteristics, blood gas chemistry, hemodynamics variables

Group characteristics are listed (Table 1). There were no differences in baseline characteristics between the Control and CO group for any of the reported variables (not shown). The variables reported are at the 2-h time point (90 min of CO exposure or room air for the Control group followed by 30 min of room air for both groups). At the 2-h time point, the CO group had significantly higher COHb levels and heart rate ($p < 0.00001$ and $p < 0.025$, respectively). Otherwise, there were no differences in other variables such as weight, mean arterial pressure and lactate.

Mitochondrial respiration

CIV-linked respiration in the CO group was significantly lower when compared to the Control group for hippocampal tissue ($p < 0.001$) but not in cortical tissue ($p = 0.12$). Brain tissue was normalized to CS activity. CIV-linked respiration for cardiac apical tissue (isolated mitochondria) was also significantly lower in the CO group when compared to the Control group ($p < 0.0001$) which was normalized to protein content (Figure 1). For both cortical and hippocampal tissue there were no differences in other states measured such as OXPHOS or LEAK. For cardiac tissue, in addition to CIV respiration, there was also a significant decrease in OXPHOS_{CI} and CII-linked and ETS_{CI} and CII-linked respiration when compared to the Control group ($p < 0.001$). All respiratory values for cortical, hippocampal, and cardiac tissue are reported (Table 2).

Reactive oxygen species generation

Mitochondrial ROS production, measured during the LEAK state and normalized to mitochondrial content (H₂O₂/mg tissue/CS) for brain tissue and protein content for heart tissue

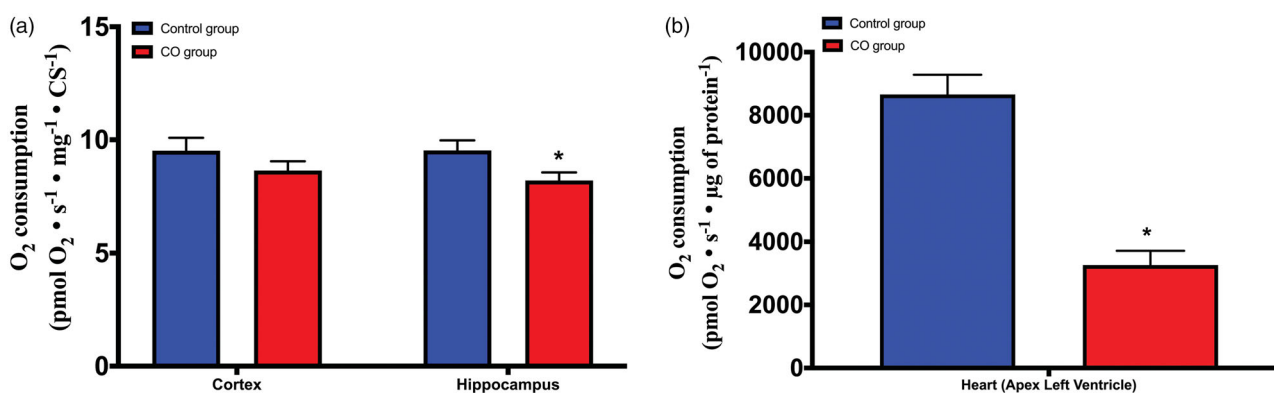


Figure 1. Brain and heart mitochondrial respiration. (A) CIV-linked respiration of cortical and hippocampal tissue. In the hippocampus, CIV-linked respiration is significantly lower in the CO group when compared to the Control group (* $p < 0.001$) but not in cortical tissue ($p = 0.12$). (B) CIV-linked respiration for cardiac tissue (isolated mitochondria) is also significantly lower in the CO group when compared to the Control group (* $p < 0.0001$). Values expressed as mean \pm SEM. CIV: Complex IV; SEM: standard error of the mean.

Table 2. Mitochondrial respiration variable.

Mitochondrial respiration (pmol O₂ • s⁻¹ • CS activity⁻¹) for brain and (pmol O₂ • s⁻¹ • protein content⁻¹) for heart

Respiratory parameters	Control			CO		
	Brain Cortex	Brain Hippocampus	Heart Apex	Brain Cortex	Brain Hippocampus	Heart Apex
OXPPOS _{CI}	2.89 \pm 0.22	2.84 \pm 0.13	5327.01 \pm 401	2.51 \pm 0.13	2.51 \pm 0.20	3236.08 \pm 415
OXPPOS _{CI+CI}	6.75 \pm 0.35	5.75 \pm 0.20	8174.84 \pm 469	6.18 \pm 0.26	5.88 \pm 0.31	5772.92 \pm 568*
LEAK	1.55 \pm 0.33	1.32 \pm 0.09	718.55 \pm 90	1.24 \pm 0.07	1.25 \pm 0.07	1038.47 \pm 67
ETS _{CI+CI}	6.88 \pm 0.20	6.50 \pm 0.23	6210.72 \pm 876	6.28 \pm 0.27	6.52 \pm 0.28	3675.04 \pm 547*
ETS _{CI}	4.18 \pm 0.09	4.17 \pm 0.23	2546.27 \pm 99	4.01 \pm 0.20	4.03 \pm 0.16	2146.57 \pm 163
CIV	9.51 \pm 0.57	9.53 \pm 0.44	8658.43 \pm 626	8.63 \pm 0.41	8.20 \pm 0.35*	3263.63 \pm 451**

Summary of mitochondrial respiration (pmol O₂ • s⁻¹ • mg⁻¹). Brain mitochondrial respiration was normalized to CS activity which is a marker of mitochondrial content. Mitochondrial respiration of isolated heart mitochondria was expressed as μg of protein. Values expressed as mean \pm SEM.

* $p < 0.001$ statistical comparison for their respective tissue between the CO group and Control group.

** $p < 0.0001$ statistical comparison for their respective tissue between the CO group and Control group.

CS: citrate synthase; OXPPOS: oxidative phosphorylation; ETS: electron transport system; C: Complex.

(H₂O₂/mg protein/CS), was significantly increased in the CO group when compared with the Control group in cortical tissue (0.051 \pm 0.003 vs 0.037 \pm 0.003, $p < 0.001$), hippocampal tissue (0.041 \pm 0.002 vs 0.03 \pm 0.001, $p < 0.001$) and cardiac apical tissue (0.316 \pm 0.027 vs 0.185 \pm 0.047, $p < 0.001$), respectively (Figure 2).

Cytokines

We measured cytokine response to CO in plasma obtained at the end of the two-hour exposure time in both groups. There was no difference in IL-1 β (0.08 \pm 0.00 vs 0.87 \pm 0.39, $p = 0.99$) or IL-6 (0.19 \pm 0.03 vs 0.39 \pm 0.16, $p > 0.99$) concentrations between the Control and CO group, respectively. There was a significant elevation in both IL-8 (10.51 \pm 2.94 vs 2.35 \pm 0.34, $p < 0.003$) and TNFa (23.04 \pm 2.29 vs 14.21 \pm 0.77, $p < 0.001$) concentrations in the CO group when compared to the Control group, respectively (Figure 3).

Cerebral microdialysis

Cerebral microdialysis (cMD) samples were taken at different times points during the 90 min exposure portion of the study. We measured the following substrates to gauge

cerebral metabolism: lactate, pyruvate, glycerol and glucose. We calculated the extracellular lactate/pyruvate ratio (LPR) which is often used as a marker of metabolic stress and may indicate mitochondrial dysfunction with a high lactate to pyruvate ratio. We compared the four animals in the Control group to four animals in the CO group (there was technical difficulty in obtaining cMD in two animals of the CO group). There was a significant increase in the LPR in the CO group compared to the Control group at 90 min (28 \pm 3.1 vs 16.7 \pm 2.2, $p < 0.006$). Both the glycerol and glucose concentrations did not differ significantly between the two groups at any of the time points measured ($p > 0.99$) (Figure 4).

Non-invasive measurement of cerebral blood flow and total hemoglobin concentration

Noninvasive optical data was collected continuously throughout the duration of each animal procedure. Prior to carbon monoxide exposure, 5 min of baseline data were recorded while the condition of the animal was stable (end tidal CO₂ = 38–42 mmHg, mean arterial pressure >45 mmHg, temperature >37.5 °C, heart rate = 80–140 bpm, SpO₂ = 92–99%). Baseline data was averaged and used to normalize subsequent data collection at timepoints of 90 min following CO

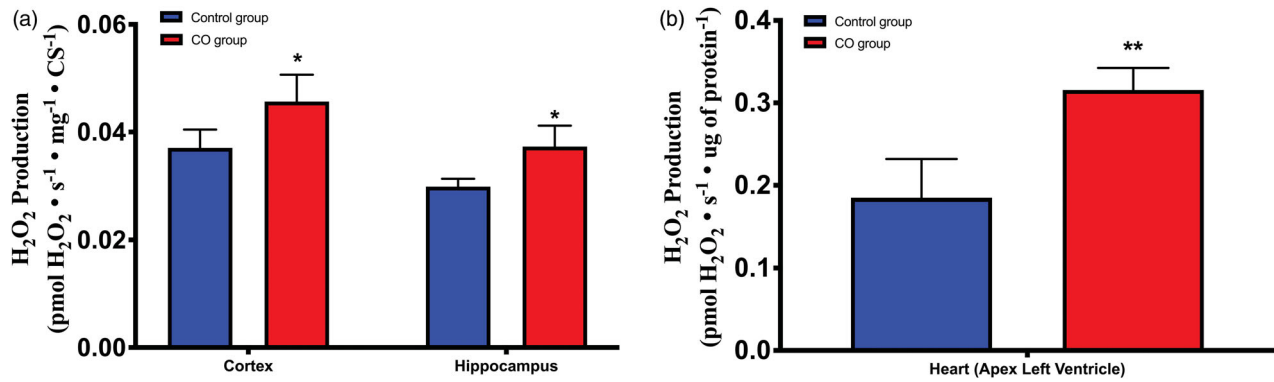


Figure 2. Mitochondrial reactive oxygen species (ROS) production. ROS is a measure of mitochondrial dysfunction with significant elevations of H₂O₂ measured as combined H₂O₂ and O₂⁻. (A) ROS is significantly increased in cortical and hippocampal tissue in the CO group when compared to the Control group (**p* < 0.001). (B) ROS is also significantly higher in the CO group when compared to the Control group (***p* < 0.001) for cardiac tissue (isolated mitochondria). Values expressed as mean ± SEM. H₂O₂: hydrogen peroxide; O₂⁻: superoxide; SEM: standard error of the mean.

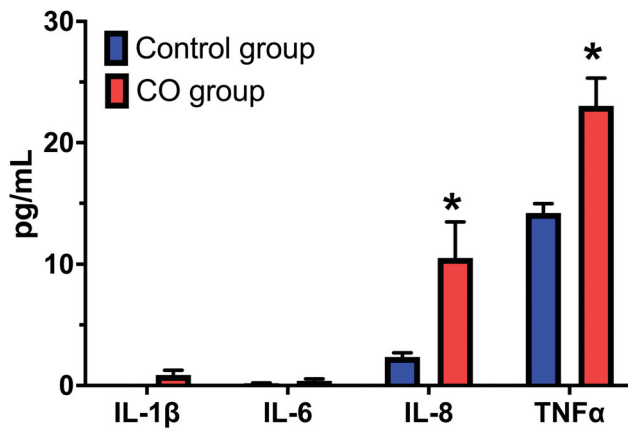


Figure 3. Plasma cytokine concentrations. There was no significant difference in IL-1β and IL-6 concentrations between the Control and the CO group in plasma obtained at the end of the 2-h exposure. Both IL-8 and TNFα concentrations were significantly increased in the CO group when compared to the Control group (**p* < 0.001). Values are expressed as mean ± SEM. IL: interleukin; TNF: tumor necrosis factor; SEM: standard error of the mean.

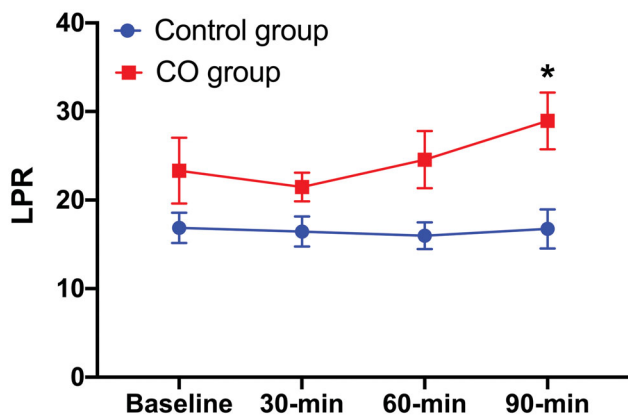


Figure 4. Cerebral microdialysis (cMD) measurements during CO exposure. Semi real-time measurements of cerebral metabolism taken at every 30 min. Cerebral LPR in the CO group was higher at 90 min when compared to the Control group (**p* < 0.006). The glycerol and glucose concentration did not significantly differ between the two groups at any time points (not shown). Values are expressed as mean ± SEM. LPR: lactate/pyruvate ratio; SEM: standard error of the mean.

exposure and 30 min following reoxygenation (Figure 5). We found increases in both cerebral blood flow (rCBF) and total hemoglobin concentration (rTHC) relative to baseline for CO

compared to Control animals. After CO exposure, the average rCBF during for the Control group was 0.67 (SD = 0.24) and that of the CO group was 1.10 (SD = 0.33) while the average rTHC for Controls was 1.09 (SD = 0.09) and CO was 1.17 (SD = 0.07). However, neither showed significant differences (rCBF between Control and CO groups had *p* = 0.055). In addition, following 30 min of reoxygenation, the average rCBF during for the Control group was 0.71 (SD = 0.32) and that of the CO group was 0.74 (SD = 0.18) while the average rTHC for the Control group was 1.11 (SD = 0.10) and CO was 1.12 (SD = 0.07).

Discussion

The objective of this study was to develop a large animal model of CO poisoning to evaluate alterations in mitochondrial function, inflammation and markers of cardiac and neurologic injury following exposure to low dose CO that mimics clinical reality. We also employed innovative non-invasive measurements of cerebral blood flow and total hemoglobin concentration. We intentionally chose a relatively low dose CO exposure to evaluate for possible subtle changes in cellular function that may be predictive of toxicity before any clinical manifestation. The overall finding was the demonstration of early mitochondrial dysfunction prior to any clinical manifestation. This would have important implications for early intervention with therapy and prognosis of CO severity. This study also provides important semi real-time evaluation of cerebral metabolism with the use of cMD to evaluate possible effects on mitochondrial function of the brain which is the organ most affected by CO.

We performed a comprehensive analysis of mitochondrial respiration and ROS generation in cortical, hippocampal and cardiac apical tissue that consistently showed CIV dysfunction (with exception of cortical tissue) even at the low dose of CO utilized in our study [7]. While CO has multiple mechanisms of action that includes hypoxia, lipid peroxidation and inflammation, its effect on mitochondrial function is less clear [26]. Our prior studies have strongly implicated the effects of CO on cellular respiration, particular at CIV with resultant cellular dysfunction [8]. In this study, there were no overt signs of clinical toxicity (with the exception of tachycardia) such as

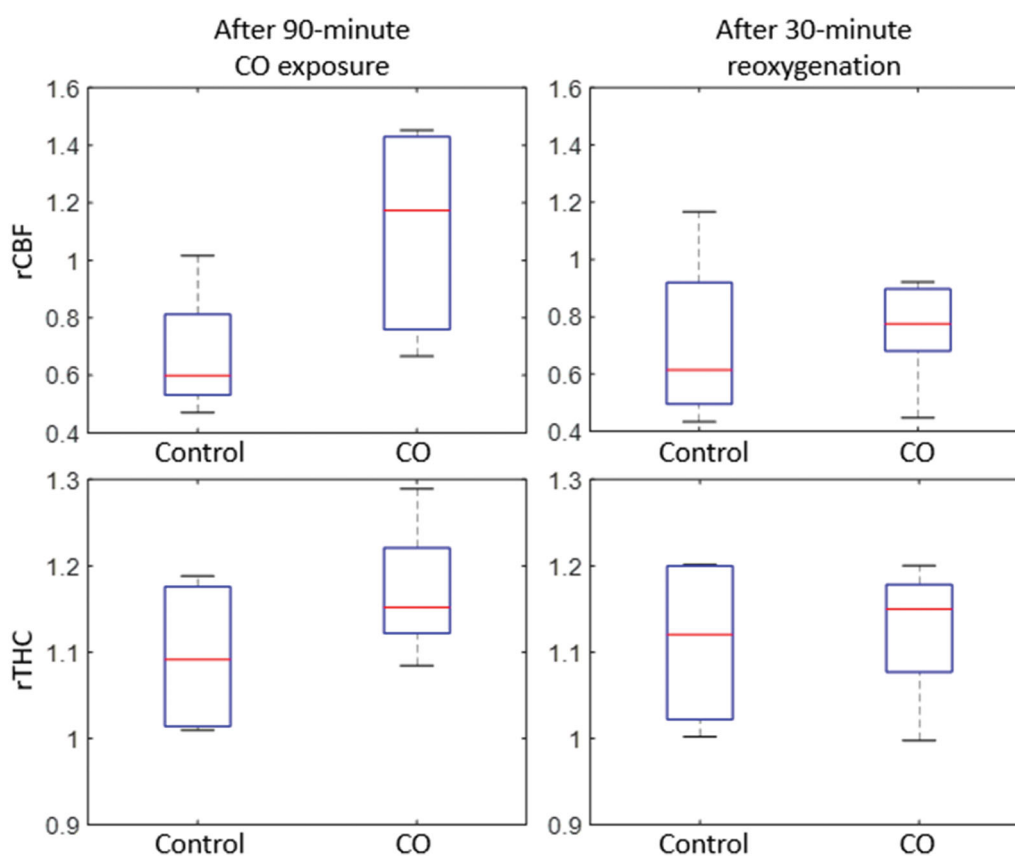


Figure 5. Non-invasive measurement of cerebral blood flow and total hemoglobin concentration. Boxplots of cerebral blood flow (rCBF) relative to baseline (top) and total hemoglobin concentration (rTHC) relative to baseline (bottom) comparing Control ($n = 4$) and CO ($n = 6$) animals 90 min following CO exposure (left) and 30 min after reoxygenation (right). On each box, the central mark indicates the median, the bottom and top edges of the box indicate the 25th and 75th percentiles, respectively, and the whiskers extend to the most extreme data points not considered outliers.

lactate generation (a marker of global cellular hypoxia) or hypotension. However, there were clear signs of mitochondrial involvement indicating early cellular injury. In addition to the cortex, we also evaluated the effects of CO on hippocampal tissue. The hippocampus is in the region of the brain that is associated primarily with memory and the regulation of emotional responses. The hippocampus is sensitive to ischemia and is commonly injured in CO poisoning leading to DNS [27,28]. Even with the low dose CO exposure we used, there was clear involvement of the hippocampal region despite no significant effects in the cortical region of the brain. We also observed the same finding of CIV inhibition in cardiac tissue similar to what was observed in the hippocampal area of the brain. Despite the lack of overt cardiac toxicity manifesting as hypotension with the exception of tachycardia, this provides further support that early cellular changes may precede clinical manifestation with either higher CO doses or duration [29]. We also obtained simultaneous measurement of ROS as combined hydrogen peroxide and superoxide using the AmR assay used in our previous works. Consistent with our findings of CIV inhibition with hippocampal and cardiac tissue we investigated; we found a significant increase in ROS in all tissue types at the 200-ppm dose we used. The main source of H_2O_2 production by mitochondria is at CIII, regulated specifically by single electron production of superoxide in the Q cycle [30]. The rate of superoxide production is enhanced by slowing the terminal

transfer rate of electrons to molecular O_2 by CO binding at CIV which may be the case in our study.

A novel aspect of this study was the use of cMD to evaluate the effect of CO on cerebral metabolism. We measured concentrations of glucose, glycerol, lactate and pyruvate across the exposure period to examine changes in cerebral metabolism related to the CIV inhibition caused by CO and increased plasma cytokine concentrations observed in our study. While there were no significant differences in both the glucose and glycerol concentrations, we calculated a lactate/pyruvate ratio (LPR) which is often an indication of dysfunction within the electron transport chain which further supports the overall mitochondrial dysfunction at the level of the brain even with the relatively low dose of CO used in our study.

Another important mediator of mitochondrial function are cytokines, small secreted proteins released by cells. Cytokines have a specific effect on the interactions and communications between cells. Over-production of cytokines have been implicated in cellular dysfunction in various disease states such as COVID-19 infections. One study used low dose of CO (50 ppm) as a treatment for inflammation induced by endotoxin in swine and found that dose of CO did not cause an increase in measured cytokine concentrations. Higher doses of CO have been shown to increase certain cytokine concentrations such as $TNF\alpha$. The decrease in mitochondrial respiration and increased ROS levels can also be attributed to

elevated cytokine concentrations in addition to CIV inhibition from CO. Studies have shown that elevated TNF α concentrations result in neurologic injury mediated from its effect on mitochondrial function [31,32].

Finally, the data collected from noninvasive optical neuro-monitoring indicate CO exposure increases cerebral blood flow as well as total hemoglobin concentration [21,33,34]. While there were no significant differences found between any optical markers comparing the Control group to CO group following CO exposure time, the trends indicate there are changes in blood flow and hemodynamics even at a relatively low dose of CO. In addition, the increase in total hemoglobin concentration may be an indication of carboxy-hemoglobin, which cannot be detected using the current optical setup. In the future, we hope to use an eight-wave-length system to attempt measurement of absolute carboxy-hemoglobin concentration.

Our study has some limitations to consider. One limitation is we used only one dose of CO exposure and future studies may employ a higher dose of CO to evaluate for a dose-dependent effect on cellular function. The same limitation can also apply to the duration of CO exposure and can also be increased for future studies. In addition to the use of 200 ppm, we arbitrarily choose a duration of 90 min followed by 30 min of room air to best mimic an acute CO exposure as opposed to a longer time period that may be more consistent with chronic CO poisoning. Another limitation is the inability to assess certain clinical manifestations of CO poisoning such as headache or dizziness given the use of swine and sedation with isoflurane. Finally, while the use of swine to model both neurological and cardiac function of humans is robust, it may not perfectly approximate the human response to CO.

In conclusion our study reveals that even at a relatively low dose of CO used there were clear alterations in cellular function that includes CIV inhibition of hippocampal and cardiac tissue along with increased ROS generation, inflammation and altered cerebral blood flow and metabolism. Our findings highlight that despite the normal physiology of swine exposed to the relatively low dose of CO, that this may represent an important pathway for therapy at the level of the mitochondria.

Disclosure statement

No potential conflict of interest was reported by the author(s).

Funding

This research was supported by the National Institutes of Health-NIH. Grant numbers K08HL136858, R21ES031243, R03HL154232 (Jang) and R01HL141386 (Kilbaugh).

ORCID

David H. Jang  <http://orcid.org/0000-0002-1213-6971>

Johannes K. Ehinger  <http://orcid.org/0000-0002-2417-5767>

Todd J. Kilbaugh  <http://orcid.org/0000-0002-4959-3092>

References

- [1] Rose JJ, Nouraie M, Gauthier MC, et al. Clinical outcomes and mortality impact of hyperbaric oxygen therapy in patients with carbon monoxide poisoning. *Crit Care Med.* 2018;46(7): e649–e655.
- [2] Gummin DD, Mowry JB, Spyker DA, et al. 2018 Annual Report of the American Association of Poison Control Centers' National Poison Data System (NPDS): 36th annual report. *Clin Toxicol (Phila).* 2019;57(12):1220–1413.
- [3] Ran T, Nurmagametov T, Sircar K. Economic implications of unintentional carbon monoxide poisoning in the United States and the cost and benefit of CO detectors. *Am J Emerg Med.* 2018;36(3):414–419.
- [4] Weaver LK, Hopkins RO, Chan KJ, et al. Hyperbaric oxygen for acute carbon monoxide poisoning. *N Engl J Med.* 2002;347(14): 1057–1067.
- [5] Gandini C, Castoldi AF, Candura SM, et al. Carbon monoxide cardiotoxicity. *J Toxicol Clin Toxicol.* 2001;39(1):35–44.
- [6] Favory R, Lancel S, Tissier S, et al. Myocardial dysfunction and potential cardiac hypoxia in rats induced by carbon monoxide inhalation. *Am J Respir Crit Care Med.* 2006;174(3):320–325.
- [7] Akyol S, Erdogan S, Idiz N, et al. The role of reactive oxygen species and oxidative stress in carbon monoxide toxicity: an in-depth analysis. *Redox Rep.* 2014;19(5):180–189.
- [8] Jang DH, Kelly M, Hardy K, et al. A preliminary study in the alterations of mitochondrial respiration in patients with carbon monoxide poisoning measured in blood cells. *Clin Toxicol (Phila).* 2017; 55(6):579–584.
- [9] Jang DH, Khatri UG, Shortal BP, et al. Alterations in mitochondrial respiration and reactive oxygen species in patients poisoned with carbon monoxide treated with hyperbaric oxygen. *ICMX.* 2018; 6(1):4.
- [10] Owiredu S, Ranganathan A, Eckmann DM, et al. Ex vivo use of cell-permeable succinate prodrug attenuates mitochondrial dysfunction in blood cells obtained from carbon monoxide-poisoned individuals. *Am J Physiol Cell Physiol.* 2020;319(1):C129–C35.
- [11] Jang DH, Greenwood JC, Spyres MB, et al. Measurement of mitochondrial respiration and motility in acute care: sepsis, trauma, and poisoning. *J Intensive Care Med.* 2017;32(1):86–94.
- [12] Chance B, Williams GR. Respiratory enzymes in oxidative phosphorylation. IV. The respiratory chain. *J Biol Chem.* 1955;217(1): 429–438.
- [13] Chance B, Williams GR, Holmes WF, et al. Respiratory enzymes in oxidative phosphorylation. V. A mechanism for oxidative phosphorylation. *J Biol Chem.* 1955;217:439–451.
- [14] Chance B, Williams GR. Respiratory enzymes in oxidative phosphorylation. VI. The effects of adenosine diphosphate on azide-treated mitochondria. *J Biol Chem.* 1956;221(1):477–489.
- [15] Brown GC. Control of respiration and ATP synthesis in mammalian mitochondria and cells. *Biochem J.* 1992;284(1):1–13.
- [16] Fredriksson K, Rooyackers O. Mitochondrial function in sepsis: respiratory versus leg muscle. *Crit Care Med.* 2007;35(9 Suppl): S449–S453.
- [17] Penney DG. Acute carbon monoxide poisoning: animal models: a review. *Toxicology.* 1990;62(2):123–160.
- [18] Helke KL, Swindle MM. Animal models of toxicology testing: the role of pigs. *Expert Opin Drug Metab Toxicol.* 2013;9(2):127–139.
- [19] Tsang HG, Rashdan NA, Whitelaw CB, et al. Large animal models of cardiovascular disease. *Cell Biochem Funct.* 2016;34(3): 113–132.
- [20] Busch DR, Balu R, Baker WB, et al. Detection of brain hypoxia based on noninvasive optical monitoring of cerebral blood flow with diffuse correlation spectroscopy. *Neurocrit Care.* 2019;30(1): 72–80.
- [21] Ko TS, Mavroudis CD, Baker WB, et al. Non-invasive optical neuro-monitoring of the temperature-dependence of cerebral oxygen metabolism during deep hypothermic cardiopulmonary bypass in neonatal swine. *J Cereb Blood Flow Metab.* 2020;40:187–203.

- [22] Durduran T, Choe R, Baker WB, et al. Diffuse optics for tissue monitoring and tomography. *Rep Prog Phys*. 2010;73:076701.
- [23] Li Z, Baker WB, Parthasarathy AB, et al. Calibration of diffuse correlation spectroscopy blood flow index with venous-occlusion diffuse optical spectroscopy in skeletal muscle. *J Biomed Opt*. 2015; 20(12):125005.
- [24] Mavroudis CD, Karlsson M, Ko T, et al. Cerebral mitochondrial dysfunction associated with deep hypothermic circulatory arrest in neonatal swine. *Eur J Cardiothorac Surg*. 2018;54(1):162–168.
- [25] Mavroudis CD, Mensah-Brown KG, Ko TS, et al. Electroencephalographic response to deep hypothermic circulatory arrest in neonatal swine and humans. *Ann Thorac Surg*. 2018;106(6):1841–1846.
- [26] Rose JJ, Wang L, Xu Q, et al. Carbon monoxide poisoning: pathogenesis, management, and future directions of therapy. *Am J Respir Crit Care Med*. 2017;195(5):596–606.
- [27] Huang YQ, Peng ZR, Huang FL, et al. Mechanism of delayed encephalopathy after acute carbon monoxide poisoning. *Neural Regen Res*. 2020;15(12):2286–2295.
- [28] Tamura T, Sugihara G, Takahashi H. Memory impairment and hippocampal volume after carbon monoxide poisoning. *Arch Clin Neuropsychol*. 2020 Aug 7;acaa050. doi: [10.1093/arclin/acaa050](https://doi.org/10.1093/arclin/acaa050).
- [29] de Jong R, van Hout GP, Houtgraaf JH, et al. Cardiac function in a long-term follow-up study of moderate and severe porcine model of chronic myocardial infarction. *Biomed Res Int*. 2015; 2015:209315.
- [30] Cadenas E, Davies KJ. Mitochondrial free radical generation, oxidative stress, and aging. *Free Radic Biol Med*. 2000;29(3–4): 222–230.
- [31] Doll DN, Rellick SL, Barr TL, et al. Rapid mitochondrial dysfunction mediates TNF-alpha-induced neurotoxicity. *J Neurochem*. 2015; 132(4):443–451.
- [32] Russell AE, Doll DN, Sarkar SN, et al. TNF-alpha and beyond: rapid mitochondrial dysfunction mediates TNF-alpha-induced neurotoxicity. *J Clin Cell Immunol*. 2016;7(6):467.
- [33] Busch DR, Baker WB, Mavroudis CD, et al. Noninvasive optical measurement of microvascular cerebral hemodynamics and autoregulation in the neonatal ECMO patient. *Pediatr Res*. 2020; 88(6):925–933.
- [34] Milej D, He L, Abdalmalak A, et al. Quantification of cerebral blood flow in adults by contrast-enhanced near-infrared spectroscopy: validation against MRI. *J Cereb Blood Flow Metab*. 2020; 40(8):1672–1684.